Effect of Chain Extenders on the Morphology Development in Flexible Polyurethane Foam

Wu Li and Anthony J. Ryan*

Department of Chemistry, University of Sheffield, Sheffield S3 7HF, UK

Ingrid K. Meier

Air Products and Chemicals, Inc., 7201 Hamilton Boulevard, Allentown, Pennsylvania 18195-1501

Received February 11, 2002; Revised Manuscript Received May 28, 2002

ABSTRACT: The effect of chain extenders on the morphology development in flexible polyurethane foam has been studied by small-angle X-ray scattering (SAXS), FTIR spectroscopy, and rheometry. Four chain extenders, diethanolamine (DEOA), 1,2-ethylene diol (EDO), glycerol, and 2-(methylamino)ethanol (MAE), were studied in a standard high-resilience (HR) foam formulation. Phase separation was observed to cause the foam modulus rise. On adding chain extenders, the onset of microphase separation was delayed, and the interdomain spacing was increased. This effect strongly depends on the chemical structure of chain extenders and the compatibility between chain extenders and urea segments. The addition of chain extenders to the formulations also delayed the onset of foam modulus growth.

Introduction

Water-blown flexible polyurethane foam is made by simultaneous chemical reactions between a diisocyanate with polyether polyol and water. Combination of these two exothermic reactions results in the formation of a multiblock copoly(urethane−urea) of the -$(H_mS)_n$- type. The carbon dioxide gas evolved from the water−isocyanate reaction blows the polymer into a foam. As the center of the foam bun is self-insulated by the surrounding polymer, the foaming process occurs under quasi-adiabatic conditions. The development of morphology during foaming is complex. As the chemical reactions proceed, the urea chain length increases and the interaction parameters (χ) between the polyether soft and polyurea hard segment also change. Such changes lead to a transition from an initial homogeneous state into a microphase-separated state at a critical conversion of isocyanate groups. The microphase-separated hard segments continue to grow, and association of these urea hard segments occurs. At the same time, strong hydrogen bonding between the urea groups can be formed within the hard domain. Microphase separation is then intercepted and quickly arrested by vitrification of the phase that is richer in hard segment. This phase has attained a composition with a glass transition temperature (T_g) equal to the temperature of the surrounding polymer medium. In summary, with branched reactants, a combination of a chemical cross-linking reaction, reaction-induced microphase separation, hydrogen-bonding formation, and vitrification occurs during the foaming process. Therefore, the resultant morphology may reflect all of these phenomena and is determined, in part, by the kinetic competition between these processes. Thus, the changes in the concentration of catalyst, cross-linker, and water will strongly affect the foam morphology development and the resulting mechanical properties.

FTIR spectroscopy has been employed to investigate both the reaction kinetics and the development of polymer structure during foam formation.[1−4] Hydrogen-bonding studies can often provide information concerning the phase separation of polyurea chains. In slabstock foam, the formation of urethane and soluble urea occurs simultaneously in the initial stages of the foaming reaction. Then the onset of a loosely ordered monodentate hydrogen-bonded urea phase occurs, followed by the initiation of the ordered, bidentate urea phase. Microphase separation of soluble urea hard-segment sequence in slabstock foams was observed to occur in the reaction at 50−60% conversion of isocyanate function groups. However, the development of the urea hard domain in high-resilience (HR) foams is not as distinct and sequential as is observed in slabstock foams. Urea microphase separation is changed as the pronounced bidentate urea phase is suppressed in the HR foam. This difference results from the chemistry of the typical components used in the different types of foam. HR foam involves a more highly reactive polyol, which has much higher ethylene oxide (EO) content and primary hydroxyl content, and the addition of a low molecular weight cross-linker which is used to improve the hardness and compression. Increasing the EO content of polyol enhances the miscibility of the urea component and other reaction components which limits the development of the urea phase.[5,6] Cross-linker was observed to seriously disrupt the hydrogen-bonding interaction and complicate the morphology development.[4] The extent of bidentate hydrogen bonding will be a function of the amount of cross-linker added.

The significance of the polyurea phase separation in relation to the rise in polymer modulus and foam stability after cell opening has been studied by rheometry.[7−10] In slabstock foam the storage modulus starts to increase at the onset of microphase separation of urea hard segments. The modulus buildup arises from the growth of the physical network of hydrogen-bonded urea hard segments. Within 5−10 s after the onset of modulus increase, cell opening normally occurs. In slabstock foam, the phase separation leads to the formation of lamellae-like polyurea domains, which can further aggregate to form larger precipitates ca. 100−300 nm in diameter.[11,12] The development of geometrically anisotropic hard domain may lead to a significant amount of connectivity and dramatically alters the properties of the solid state. Increasing

10.1021/ma020231l CCC: $22.00 © 2002 American Chemical Society
Published on Web 06/28/2002

Table 1. Details of the Polyurethane Foam Formulations

component (part by weight)	DEOA	no additive	glycerol	EDO	MAE
Hyperlite E824	74.0	74.0	74.0	74.0	74.0
Hyperlite E852	26.0	26.0	26.0	26.0	26.0
Dabco DC5043	0.75	0.75	0.75	0.75	0.75
Dabco DC5169	0.25	0.25	0.25	0.25	0.25
Dabco BL11	0.08	0.08	0.08	0.08	0.08
Dabco 33LV	0.30	0.30	0.30	0.30	0.30
chain extender	1.49		1.32	1.32	1.57
water	3.5	3.5	3.5	3.5	3.5
Voranate T80	44.8	40.7	44.8	44.8	44.8

interconnectivity between the hard domains may lead to a much higher modulus than a foam polymer with a dispersed hard domain morphology. When cross-linker DEOA is added to the formulation, the hard domains become smaller and more geometrically isotropic, and those larger precipitates cannot typically be observed in HR foam. The level of hard domain interconnectivity may thus be reduced, which results in the reduction in the foam modulus.[11]

The small-angle X-ray scattering (SAXS) technique has been used to investigate the phase separation kinetics during the foaming process.[3,13] In Ryan and Elwell's[13] dynamic IR and SAXS studies of a methylene diphenyl diisocyanate (MDI) slabstock foam system, a close agreement between the onset of microphase separation detected by FTIR spectroscopy and SAXS was observed. Similar results have also been reported by McClusky[3] for a toluene diisocyanate (TDI) slabstock foam system. In TDI-based molded foam, it was observed that the amount of bidentate urea was not an accurate indicator of the amount of phase separation. The cross-linker, diethanolamine (DEOA), was shown to increase the number of hard domains and alter the hard domain formation time dramatically.

In this paper, four chain extenders, diethanolamine (DEOA), 1,2-ethylene diol (EDO), glycerol, and 2-methylaminoethanol (MAE), are studied in a standard TDI HR polyurethane foam formulation. A HR foam without any chain extender was tested as a reference. Reaction kinetics were measured by adiabatic temperature rise measurements, and the effects of chain extenders on the morphology developments were investigated in situ using synchrotron SAXS, FTIR spectroscopy, and rheometry.

Experimental Section

Materials. Four chain extenders, DEOA, EDO, glycerol, and MAE, were used in this study. The number of equivalents of each chain extender in the formulation was kept the same. Formulation details are listed in Table 1. An isocyanate index of 105 and a water concentration of 3.5 g per 100 g of polyol were maintained throughout the work. Voranate T-80 (Dow Chemical) is an 80:20 mixture of the 2,4- and 2,6-isomers of toluene diisocyanate (TDI). The polyol Hyperlite E824 (Arco Chemical) is nominally a triol containing 78% propylene oxide and 22% ethylene oxide with terminal primary hydroxyl groups. Hyperlite E852 (Arco Chemical) is a poly(styrene−acrylonitrile)-filled polyol containing 80% propylene oxide and 20% ethylene oxide. The catalysts employed were DABCO 33LV and BL11 (Air Products and Chemicals); the surfactants used were DABCO DC5043 and DC5169 (Air Products and Chemicals). Polyol, surfactant, water, tertiary amine catalysts, and optional additives were weighed into a 1 L paper cup and mixed at 5000 rpm for 8 s using a Heidolph mechanical mixer. The preweighed TDI was added, and the mixture was stirred at 5000 rpm for an additional 6 s. The reacting material was then transferred to the appropriate reaction vessel.

Adiabatic Temperature Rise Measurements. The reactant mixture was poured into a 1 L paper cup insulated by a block of flexible polyurethane foam to perform the temperature rise measurement. A type K thermocouple (0.25 mm diameter, TC Ltd.) was positioned in the center of the paper cup with the tip 6 cm above the base. Thermocouple temperatures as a function of time were recorded at a rate of 1 Hz using a 586 personal computer equipped with Strawberry Tree Datashuttle data acquisition hardware and a Workbench 3.00 software package.

FTIR Spectroscopy. The IR data were collected using the attenuated total reflectance (ATR) technique. A 45° single bounce zinc selenide (ZnSe) crystal with a circular surface of 20 mm diameter was embedded in the wall of an aluminum block which was fitted with 400 W heating capacity. The temperatures were recorded and controlled for 1000 s at a frequency of 1 Hz using a 586 personal computer equipped with Strawberry Tree Datashuttle data acquisition hardware running Workbench 3.00 software package. Infrared spectra were collected at 4 cm^{-1} resolution, co-adding 5 scans per file, on an ATI Mattson Galaxy 2020 series FT-IR spectrometer. Scanning time was about 7 s per file. Infrared data for the background file were obtained at 4 cm^{-1} resolution, co-adding 32 scans, prior to the execution of a kinetic run. Winfirst software (Analytical Technology, Inc.) was used for all of the computer data assisted acquisition and subsequent data analysis.

Rheometry. The modulus development during foaming was measured using a vane rheometer.[14] Four blades made of 1 mm thick iron slides were fused onto a central iron shaft. The blades were 25 mm high, and the overall diameter was 55 mm. The whole vane fixture was coated with a layer of poly(tetrafluoroethylene) (PTFE) film and attached via an adapter to a Rheometrics SR-5000 stress-controlled rheometer. The outside container was a stiff polypropylene beaker with the diameter of 110 mm at the level of the blades. The bottom of the vane fixture was 45 mm from the bottom of the beaker. The foaming mixture was poured into a polypropylene beaker that was then mounted on the rheometer with the vane fixture and allowed to react. To obtain the modulus value of the reactive foam, a frequency of 10 rads/s and a strain of 0.01 were used. Data acquisition time was zeroed from the start of the final 6 s of mixing. Data were not collected during the first 30 s, which allowed the foam to rise above the height of the vane. Then the data were collected every 2 s over a period of 1000 s.

Synchrotron SAXS. SAXS measurements were conducted on beamline 16.1 at the Synchrotron Radiation Source (SRS) at the SERC Daresbury Laboratory, Warrington, UK, using 1.41 Å wavelength X-rays. A multiwire area RAPID fast detector was used at a sample distance of 3.5 m, and data were collected every 3 s over a period of 765 s. A static mixer apparatus was employed to remotely mix and inject the reaction mixture into a temperature-controlled SAXS reaction cell. The specifications of the SAXS sample cell, the experimental arrangement, and the procedures adopted are described elsewhere.[15]

Results and Discussion

Foam Reaction Kinetics Tests. Assuming that there are no side reactions, the only source of heat during the foaming reaction arises from consumption of the isocyanate functional groups. It is thus possible to correlate the foam temperature to the isocyanate conversion. The fractional isocyanate conversion is estimated by the following expression:[16,17]

$$P_{NCO} = \frac{r(T_t - T_0)}{T_{ad,calc}} \quad (1)$$

where r is the stoichiometric ratio of total hydroxyl equivalents to isocyanate equivalents, T_t is the foam

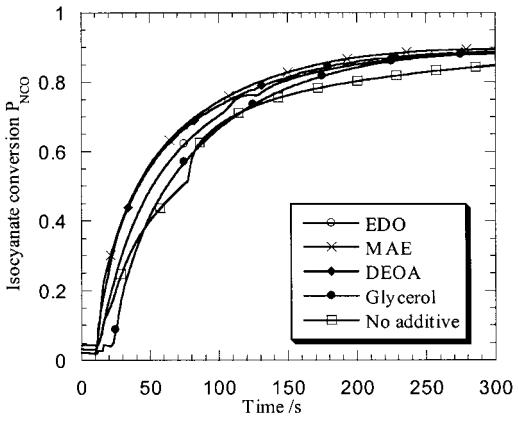

Figure 1. Isocyanate conversion P_{NCO} vs time for the foaming systems studied.

temperature at time t, T_0 is the initial temperature of reacting mixture, and $\Delta T_{ad,calc}$ is the calculated adiabatic temperature rise. Figure 1 illustrates the isocyanate conversion vs time for the foaming systems investigated. The additives diethanolamine and 2-methylaminoethanol contain reactive amine groups which react faster than the primary hydroxyl group. They also have some catalytic activity. Thus, the DEOA and MAE systems have a higher isocyanate conversion in the early part of the foaming reaction than the glycerol and EDO systems do.

Because it contains approximately 10% less active hydrogen, the foam with no chain extender has the lowest rate of reaction of all of the foaming systems. The foam cells were observed to open at 74 s, and then the foam collapsed. From the isocyanate conversion profile, an apparent acceleration in the rate of reaction was clearly observed to occur at 77 s. The apparent acceleration in the rate of reaction observed here might have been a consequence of the foam collapse that was induced by urea segregation.

FTIR Spectroscopy. Because they can be correlated to morphological features, inter-urea and inter-urethane hydrogen bonding are frequently used to study the degree of phase separation. In the infrared analysis of hydrogen bonding, three spectral regions have been studied: (1) the N−H stretching region between 3500 and 3200 cm^{-1}, (2) the carbonyl region between 1800 and 1600 cm^{-1}, and (3) the amide II region below 1600 cm^{-1}.[3,18−22] Because of the variations in extinction coefficient with hydrogen bonding in the N−H stretching region and the generally complex nature of the peaks in the amide II region, only the carbonyl region has been chosen to monitor the evolution of urethane, urea, and hydrogen bonding. The formation of hydrogen bonds results in a shift of the absorption band of the C═O stretching vibration mode from a higher frequency value to a lower one. The exact new position depends very much on the strength of the hydrogen bonds that form, and this bond strength strongly depends on the local geometry, particularly the linearity of the bonds involved and the distance between the groups.[18,23,24] A summary of the frequency assignments to the specific functional groups, interactions, and types of hydrogen bonding is presented in Table 2.

Figure 2 shows the development of the absorbance in the carbonyl region for foam with no chain extender. Both free urethane and soluble urea are evolved at an early point in the reaction. The free urethane occurred as a shoulder of the broad soluble urea peak at 1715 cm^{-1}, while the hydrogen-bonded urethane cannot be observed which might be due to its low concentration. The intensity in the region of 1660−1700 cm^{-1} (the monodentate urea phase) starts to increase at 47 s. Then the pronounced bidentate urea band suddenly appears at 69 s, and its intensity develops very quickly. Bidentate urea is the microphase-separated, hydrogen-bonded urea. The onset of microphase separation is taken as the point at which there is an acceleration in the intensity of bidentate urea. For foam with no additive, the microphase separation occurs at 69 ± 3 s, and the corresponding isocyanate conversion is 0.52 ± 0.03. Artavia[1] and Elwell[2] observed that the microphase separation occurred at a critical isocyanate conversion at which the local number-average hard-segment sequence length, N_H, reaches a critical sequence length, N_{Hcrit}, which is no longer thermodynamically compatible with the surrounding phase. The critical value of isocyanate conversion for slabstock foams with the water concentration from 2.1 to 5.4% is approximately 0.55 ± 0.05,[1,2] which is the same as the value observed here, although different kinds of polyol and catalyst were used in this foaming system.

Table 2. Infrared Band Assignments for Polyurethane Foams

wavenumber (cm^{-1})	band assignment
1730	free urethane
1715	soluble urea
1700−1650	monodentate urea (disordered H-bonded urea)
1640	bidentate urea (ordered H-bonded urea)
1710−1700	H-bonded urethane

Adding chain extenders to the formulations seriously alters the formation of urea hydrogen bonds. On adding EDO and glycerol, the development of the bidentate urea can also be clearly observed. However, the development of the monodentate urea is stronger than that of foam with no additive. Finally, a broad peak with its peak position at 1640 cm^{-1}, which covers both the monodentate and bidentate urea region, is formed. The bidentate urea develops quite weakly in MAE foam and becomes a shoulder of the broad peak of monodentate urea. On adding DEOA, the bidentate urea is seriously suppressed. Disordered hard domains are formed in the foam made with DEOA and MAE. For the foam with chain extender, the amount of bidentate urea is no longer an accurate indication of the amount of phase segregation. The final spectra in the carbonyl region for all foam systems are plotted in Figure 3.

Wide-angle X-ray scattering (WAXS) patterns of the PU foams indicate urea and hard-segment ordering that may be of a paracrystalline nature but certainly lacking in true 3-dimensional crystallinity.[12] Using wide-angle X-ray scattering (WAXS), Dounis[25] observed that the amorphous character of the hard segment domains was much more pronounced as the DEOA content was increased. The chain extenders disrupt the paracrystalline packing of the urea groups and the ordering of the hydrogen-bonding interactions in the hard domains. This disruption occurs because the chain extenders change the hard-segment structure, precluding the development of local ordering and altering the composition of the hydrogen-bonded species.[11,26,27] During the microphase separation process, the soft segments and other impurities will be excluded from hard domains. The more the impurities are excluded, the less disrupted the hard domains and the stronger the bidentate urea

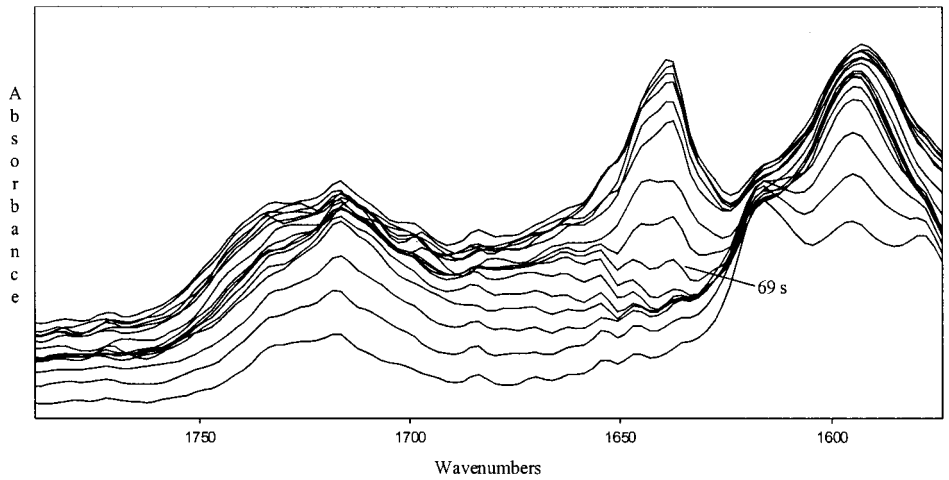

Figure 2. Plot illustrating the development of the peaks in the carbonyl region for foam with no chain extender every 7.5 s from 25 s. Note the rapid growth of bidentate urea at 1640 cm^{-1}.

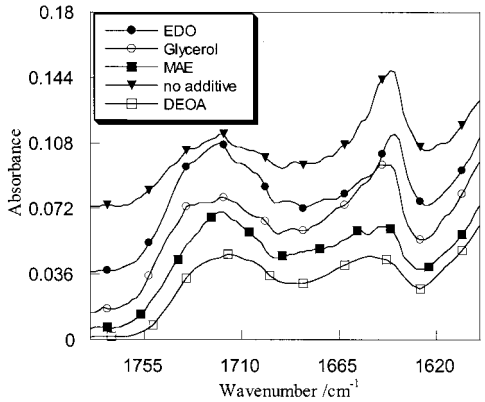

Figure 3. Plot of final spectra in the carbonyl region for all foaming systems.

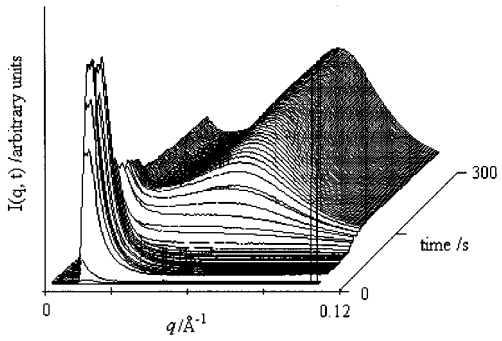

Figure 4. Three-dimensional plot of $I(q,t)$, vs q, vs t, for a representative data set for DEOA-containing foam.

hydrogen bonding will be. DEOA and MAE can form urea linkages that are chemically similar to and very compatible with the hard domains that result from the reaction of water and diisocyanate. The higher degree of precipitation of DEOA and MAE inside the urea hard domains is confirmed by the larger interdomain spacing observed in SAXS experiments. Comparison of the development of peaks in the carbonyl region reveals that the degree of disruption in urea packing and hydrogen-bonding interactions by the chain extenders decreases in the order DEOA > MAE > glycerol > EDO.

The stronger the interaction between the urea segments is, the less soluble the urea segments and the higher the driving force for hard domain formation will be. Thus, the disruption of the hydrogen-bonding interaction by the chain extenders will strongly affect the phase separation. FTIR spectroscopy is an indirect method of measuring the microphase separation process during the foaming reaction, and thus, it cannot be used here for HR foam. The effect of the chain extenders on hard domain formation needs to be investigated by SAXS, which probes the electron density differences directly.

Synchrotron SAXS. Figure 4 shows representative three-dimensional plots of intensity, $I(q,t)$, vs scattering vector, q, vs time, t, for DEOA-containing foam. An initial upturn in $I(q)$ at low q is observed. This appears to be due to the filling of the cell with a liquid mixture that contains microvoids. The change in the volume fraction of the bubbles during the reaction contributes to the upturn in $I(q)$.[13] No scattering peak can be observed in the early stage of the reaction. The liquid mixture, which is comprised of unreacted monomer, urea hard-segment chain and isocyanate-tipped polyether oligomers, is homogeneous at this stage. After 75 ± 3 s, there is the first appearance of a scattering maxima at $q \approx 0.06$ $Å^{-1}$, which indicates the onset of microphase separation. The peak intensity increases rapidly up to approximately 120 s, after which the growth of peak intensity slows down and eventually becomes approximately constant. At this time, microphase separation is intercepted and quickly arrested by vitrification of the phase that is richer in hard segments. This phase has attained a composition with a T_g equal to the temperature of the surrounding polymer medium.

The development of total scattered intensity, or invariant Q, can be employed to characterize the structural development as well as the degree of microphase separation: an increase in invariant Q corresponds to an increase in the degree of phase separation. The invariant is independent of the size or spatial arrangement of the structural inhomogeneities and is expressed as[28]

$$Q = \int_0^\infty I(q)q^2\,\mathrm{d}q \sim \phi_1\phi_2(\rho_1 - \rho_2)^2 \qquad (2)$$

where ρ_i and ϕ_i are the electron density and volume fraction, respectively. In this study, a relative invariant Q' is calculated from the arbitrary intensity experimental data by summation of the area under the $I(q)q^2$ vs q curve between the first reliable data point at $q = 0.02$

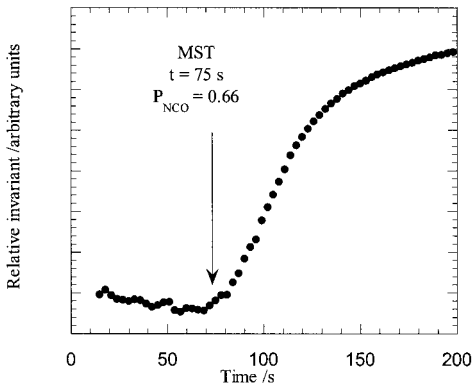

Figure 5. Plot of the relative invariant Q' as a function of time for DEOA-containing foam.

$Å^{-1}$ and the region in which $I(q)q^2$ becomes constant at $q = 0.12$ $Å^{-1}$. The relative invariant represents the biggest contribution to the magnitude of Q and gives a quantitative indication of the relative electron density fluctuations.

Figure 5 illustrates a plot of the relative invariant as a function of time for the DEOA-containing foam system. The cause of the initial decrease in the relative invariant is thought to be due to the contribution to Q' from microvoid (bubble) scattering.[13] The onset of microphase separation is taken as the point at which Q' starts to increase rapidly. From the plot it is apparent that the onset of microphase separation occurs at 75 s, which corresponds to an isocyanate conversion $P_{NCO} = 0.66 \pm 0.02$. The time at the onset of microphase separation and the corresponding isocyanate conversion (calculated from the ATR method) for the different foam systems are presented in Table 3. From these results it is clear that the chain extenders delay the onset of microphase separation. Although the same molar concentration of chain extender is used in each formulation, the resultant delay in the time and isocyanate conversion at the onset of microphase separation differs depending on the chain extender used. The onset of microphase separation in foam with no chain extender was observed to occur at 69 ± 3 s and 0.52 ± 0.02 isocyanate conversion. EDO increased the isocyanate conversion at the onset of microphase separation to 0.60 ± 0.02. DEOA, MAE, and glycerol further increased the isocyanate conversion at the onset of microphase separation to 0.66 ± 0.03. At the onset of microphase separation, the foam systems mainly comprise polyether, polyurea, and polyether−polyurea block copolymer that contains a urethane linking group; these mixtures are similar to ternary polymer blends. The microphase separation of urea segments has been observed to proceed via a spinodal decomposition mechanism and to yield a bicontinuous morphology.[2,7,8,10,13,15] There have been a large number of studies of the morphology and properties of polyurethane foams, and different research groups have observed particulate[5,11,25−27] and continuous[2,10,13,17] hard-segment structures in a wide range of formulations. Our concern here is the initial development of structure which follows spinodal kinetics. The final morphology of the material is dependent on a wide range of factors, and modeling of the scattering from these structures gives a good fit to a bicontinuous microemulsion structure factor. A recent AFM study[29] showed that connected structure can arise in polyurethane, and this is supported by our earlier work[30,31] and recent SAXS and AFM studies.[15]

The final one-dimensional Bragg (1-d) spacing for each system is also shown in Table 3. This value is estimated from q^*, corresponding to the maximum of the $I(q)q^2$ vs q plot, using Bragg's equation. With the exception of the chain extender-free system, the interdomain spacings for these foam systems were quite different, even though they contained the same hard-segment volume fraction (ϕ_{HS}). The foam with no chain extender had both the lowest hard-segment volume fraction and the smallest 1-d spacing, 76 Å. The addition of chain extenders to the formulation increased the interdomain spacing. EDO and glycerol slightly increased the interdomain spacing to 81 and 84 Å, respectively. The DEOA- and MAE-containing foam systems both had the largest 1-d spacing, 93 Å. The increased interdomain spacing is due to the formation of larger hard domains that result from the precipitation of the chain extenders. The difference in the 1-d spacing may be due to the increased compatibility of the DEOA−urea and MAE−urea linkages that can phase separate concurrently with the urea hard domains that are formed via the water/diisocyanate reaction. Thus, most of the DEOA and MAE can precipitate within the urea hard domains during the microphase separation process. The low reactivity of EDO and glycerol may also be responsible for preventing some portion of those chain extenders from reacting completely at the time of microphase separation. The unreacted EDO and glycerol will remain in the soft domains. The precipitation of chain extenders within the urea hard domain will interfere with hard-segment packing, leading to the breakup of long-range ordering of hydrogen-bonded species that has been observed in the FTIR experiments. The larger the interdomain spacing, the higher the content of chain extender inside the hard domain and the more disordered the hard domain will be.

The driving force for microphase separation is the large difference in solubility between the hard- and soft-segment blocks. As the polymerization proceeds, the degree of polymerization of hard-segment (N_H) increases, and the interaction parameter (χ) also changes. At a particular conversion of isocyanate groups, the number-average hard-segment sequence length reaches a critical value, and the product, χN_H, is such that the system is no longer thermodynamically stable. The polymerization acts as a thermodynamic quench, and the phase separation takes place under successive increases in quench depth. The chain extenders change the hard-segment structure and alter the ordering of the hydrogen-bonding interactions by linking to the urea formed by the water/isocyanate reaction. Such changes cause a decrease in the intradomain cohesion of hard segments and an increase in the compatibility between the soft- and hard-segment blocks. As the value of χ decreases, a larger value of N_H is required for the system to reach the same minimum thermodynamic quench depth, resulting in the delay of the onset of microphase separation. DEOA, glycerol, and MAE cause the microphase separation to occur at a higher isocyanate conversion than EDO does. Although DEOA has three reactive hydrogens while MEA has only two, the onset of microphase separation in both the DEOA and MAE foam systems occurs at the same time. The delay in the onset of microphase separation results from the change in the value of χ rather than from the formation of covalent cross-linking networks.

Table 3. Rheological and SAXS Characteristics of the Various Foaming Systems

	onset of physical gelation		onset of phase separation			
foaming system	time/s	P_{NCO}	time/s	P_{NCO}	1-d/Å	ϕ_{HS}[a]
no additive	70 ± 4	0.52 ± 0.03	68 ± 3	0.52 ± 0.02	76 ± 2	22
DEOA	80 ± 2	0.68 ± 0.02	78 ± 3	0.67 ± 0.02	93 ± 2	24
MAE	84 ± 2	0.70 ± 0.02	78 ± 3	0.68 ± 0.02	93 ± 2	24
glycerol	102 ± 4	0.67 ± 0.02	100 ± 3	0.66 ± 0.01	84 ± 1	24
EDO	71 ± 2	0.61 ± 0.02	69 ± 3	0.60 ± 0.02	81 ± 2	24

[a] Assuming hard-segment formation from both water−TDI and chain extender−TDI reactions.

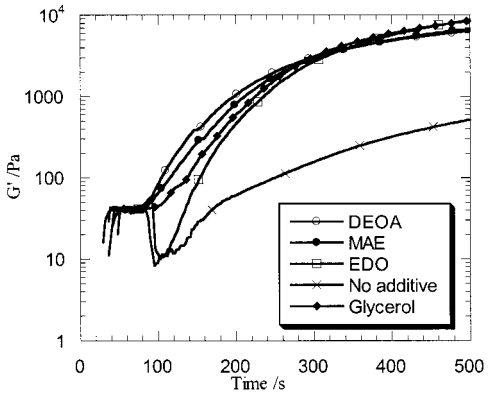

Figure 6. Shear modulus G' development profiles for all foaming systems.

Dynamic Rheometry. The modulus development within foams made using different chain extenders shows a very important trend, as can be seen in Figure 6. Three of the four distinct regions of rheological development that have been previously observed during the formation of polyurethane foam by Mora,[8] Neff,[7] and Elwell[17] are observed here: (1) bubble network or liquid foam, (2) urea microphase separation, and (3) final curing. Note that, within experimental error, the magnitude of the plateau region is unaffected by a change in chain extender. For foam made with no chain extender or using EDO, the foam cells opened, and the foam collapsed 5 or 10 s after the growth of G'; therefore; it was not possible to measure a realistic foam modulus after physical gelation. The increase in the apparent G' again after the foam collapse is due to an increase in G' of the collapsed polymer, resulting from microphase separation and vitrification of urea hard-segment domains. The sudden stiffening of the polymer in the absence of a covalent network results in a brittle material that cannot accommodate the additional strain required by continued expansion of the foam. Thus, the cell windows rupture and blow-off occurs. If the polymer foam is too weak to support its weight after cell windows rupture, the foam will collapse. No blow-off or cell opening can be observed for the DEOA, MAE, or glycerol foam systems. Neff[7] has suggested that cross-linkers could substantially increase the extensibility of the foam polymer by the earlier formation of covalent networks, thus allowing the cell windows to accommodate more strain and not break when the polymer foam stiffens. Both MAE and EDO decrease the average functionality of the foaming system, and the covalent network is formed later than that of foam with no chain extender. If this hypothesis is correct, the MAE foam should collapse in a manner similar to the foams prepared with no chain extender and EDO.

From the data in Table 3, an excellent correlation between the onset of microphase separation and modulus growth is observed for all foaming systems, clearly suggesting that the microphase separation process leads to the modulus increase and cell opening. This observation conflicts with McClusky[3] and Zhang's[32] suggestion that the gelling reaction builds up the network structure and that those chemical cross-links will cause the modulus rise in molded foam systems. If the formation of covalent networks causes the modulus rise, the modulus development profile of MAE and DEOA should be significantly different. Instead, MAE and DEOA have the same modulus development profile. Compared with foams prepared with no chain extender and EDO, the DEOA, MAE, and glycerol foam systems have higher isocyanate conversions at the onset of physical gelation as the result of the delayed microphase separation process.

However, the urea physical network does not provide all the strength needed to support the foamed polymer. The foam with no chain extender collapses after cell opening although strong bidentate urea is formed. During phase separation, a bicontinuous morphology is formed via spinodal decomposition. At this time, the foaming system mainly comprises polyether, polyurea, and polyether−polyurea block copolymer that contains a urethane linking group. On adding DEOA, MAE, and glycerol, the microphase separation is delayed, and more block copolymer can be formed. The compatibility and connectivity between the hard- and soft-segment domains are increased. By increasing the connectivity between the hard- and soft-segment domains, the stress on the urea physical network can be spread to the soft phase and thus increase the extensibility and the strength of the foamed polymer. The delay in the onset of microphase separation that results from the use of multifunctional chain extenders leads to an increase in the molecular weight of polyether at the time of cell opening. The increase in the molecular weight significantly increases the viscosity of the foamed polymer, which results in a higher degree of closed cell foam.

Conclusion

By adding chain extenders to high-resilience flexible polyurethane foam systems, the onset of microphase separation can be delayed and the interdomain spacing increased. This occurs because the chain extenders precipitate in the hard domains, change the hard segment structure, and alter the ordering of the hydrogen bonding. Such changes decrease the intradomain cohesion of hard segments and increase the compatibility between the soft- and hard-segment blocks. This effect strongly depends on the chemical structure of the chain extenders and the compatibility between chain extenders and urea segments. The higher the functionality and the better the compatibility with the hard domains, the greater the disruption in order will be. The degree of disruption caused by the chain extenders in this study was found to decrease in the order DEOA > MAE > glycerol > EDO.

Phase separation causes the foam modulus to rise. Cell opening is observed to occur a few seconds after the onset of G' growth, and it is triggered by the microphase separation which dramatically changes the rheology of the polymer. The degree of cell opening is strongly controlled by the strength of the polymer foam. The addition of chain extenders to the formulations alters the microphase separation process and increases the connectivity between the soft- and hard-segment domains. These changes delay the onset of G' growth and increase the strength of the polymer foam, resulting in the increase of number of closed foam cells.

Acknowledgment. This work was financially supported by Air Products & Chemicals, Ltd. Ellen Heeley and Anthony Gleeson assisted in the collection of SAXS data. The SAXS cell and control electronics were constructed by Chris Lumley, Mike Carr, and Paul Turner.

References and Notes

(1) Artavia, L. D.; Macosko, C. W. In *Proceedings of the 33rd SPI Annual Technical & Marketing Conference*; Technomic Publishing Co.: Lancaster, PA, 1990.
(2) Elwell, M. J.; Ryan, A. J.; Grunbauer, H. J. M.; VanLieshout, H. C. *Polymer* **1996**, *37*, 1353−1361.
(3) McClusky, J. V.; Priester, R. D.; O'Neill, R. E.; Willkomm, W. R.; Heaney, M. D.; Capel, M. A. *J. Cell. Plast.* **1994**, *30*, 338−360.
(4) Priester, R. D.; McCluskey, J. V.; O'Neill, R. E.; Turner, R. B.; Harthcock, M. A.; Davis, B. L. *J. Cell. Plast.* **1990**, *26*, 346−365.
(5) Kaushiva, B. D.; McCartney, S. R.; Rossmy, G. R.; Wilkes, G. L. *Polymer* **2000**, *41*, 285−310.
(6) Creswick, M. W.; Lee, K. D.; Turner, R. B.; Huber, L. M. *J. Elastomer Plast.* **1989**, *21*, 179−196.
(7) Neff, R.; Macosko, C. W. In *35th Annual Polyurethane Technical/Marketing Conference*, 1994.
(8) Mora, E.; Artavia, L. D.; Macosko, C. W. *J. Rheol.* **1991**, *35*, 921−940.
(9) McCluskey, J. V.; O'Neill, R. E.; Priester, R. D.; Ramsey, W. A. *J. Cell. Plast.* **1994**, *30*, 224−241.
(10) Elwell, M. J.; Ryan, A. J.; Grunbauer, H. J. M.; VanLieshout, H. C. *Macromolecules* **1996**, *29*, 2960−2968.
(11) Kaushiva, B. D.; Wilkes, G. L. *Polymer* **2000**, *41*, 6981−6986.
(12) Armistead, J. P.; Wilkes, G. L.; Turner, R. B. *J. Appl. Polym. Sci.* **1988**, *35*, 601−629.
(13) Elwell, M. J.; Mortimer, S.; Ryan, A. J. *Macromolecules* **1994**, *27*, 5428−5439.
(14) Zhang, X. D.; Giles, D. W.; Barocas, V. H.; Yasunaga, K.; Macosko, C. W. *J. Rheol.* **1998**, *42*, 871−889.
(15) Li, W.; Ryan, A. J.; Meier, I. K. *Macromolecules* **2002**, *35*, 5034−5042.
(16) Pannone, M. C. MSc, University of Minnesota, 1985.
(17) Elwell, M. J. Ph.D., University of Manchester, 1993.
(18) Sung, C. S. P.; Schneider, N. S. *Macromolecules* **1975**, *8*, 68−73.
(19) Coleman, M. M.; Lee, K. H.; Skrovanek, D. J.; Painter, P. C. *Macromolecules* **1986**, *19*, 2149−2157.
(20) Coleman, M. M.; Skrovanek, D. J.; Hu, J. B.; Painter, P. C. *Macromolecules* **1988**, *21*, 59−65.
(21) Skrovanek, D. J.; Painter, P. C.; Coleman, M. M. *Macromolecules* **1986**, *19*, 699−705.
(22) Skrovanek, D. J.; Howe, S. E.; Painter, P. C.; Coleman, M. M. *Macromolecules* **1985**, *18*, 1676−1683.
(23) Pimentel, G. L.; Sederholm, C. H. *J. Chem. Phys.* **1956**, *24*, 639.
(24) Cheam, T. C.; Krimm, S. *J. Mol. Struct.* **1986**, *146*, 175−189.
(25) Dounis, D. V.; Wilkes, G. L. *J. Appl. Polym. Sci.* **1997**, *65*, 525−537.
(26) Kaushiva, B. D.; Wilkes, G. L. *J. Appl. Polym. Sci.* **2000**, *77*, 202−216.
(27) Kaushiva, B. D.; Wilkes, G. L. *Polym. Commun.* **2000**, *41*, 6981−6986.
(28) Glatter, O., Kratky, O., Eds.; *Small-Angle X-ray Scattering*; Academic Press: London, 1983.
(29) Garrett, J. T.; Siedlecki, C. A.; Runt, J. *Macromolecules* **2000**, *34*, 7066−7070.
(30) Hamley, I. W.; Stanford, J. L.; Wilkinson, A. N.; Elwell, M. J.; Ryan, A. J. *Polymer* **2000**, *41*, 2569−2576.
(31) Hamley, I. W. *Macromol. Theory Simul.* **2000**, *9*, 363−380.
(32) Zhang, X. D.; Bertsch, L. M.; Macosko, C. W.; Turner, R. B.; House, D. W.; Scott, R. V. *Cell Polym.* **1998**, *17*, 327−349.

MA020231L